

Influence of spectral acceleration correlation models on conditional mean spectra and probabilistic seismic hazard analysis

Ali Rodríguez-Castellanos¹  | Sonia E. Ruiz¹  | Edén Bojórquez²  |
Alfredo Reyes-Salazar² 

¹Instituto de Ingeniería, Universidad Nacional Autónoma de México, Ciudad Universitaria Coyoacán, Mexico City, 04510, Mexico

²Facultad de Ingeniería, Universidad Autónoma de Sinaloa, Calzada de las Américas y B. Universitarios s/n, Culiacan, Sinaloa, 80040, Mexico

Correspondence

Sonia E. Ruiz, Instituto de Ingeniería, Universidad Nacional Autónoma de México, Copyacan, C.P. 04510, Mexico City, Mexico.
Email: sruizg@iingen.unam.mx

Summary

Innovative engineering applications are proposed to satisfy the current necessities of earthquake engineering, which are well established from a conceptual perspective, and frequently, the development of some missing inputs is only required to employ them, such as the case of the correlations between spectral values at different vibration periods. Accordingly, we computed the correlation between spectral accelerations at two vibration periods using ground motions from interplate and, alternatively, intraslab events, recorded in firm ground of Mexico City. Results show that the spreading of correlation values depends on the rupture mechanism. Then, based on hypothesis test analyses, we used four correlation models available in the literature to predict our correlation values. According to the findings, we proposed a predictive correlation mathematical model for interplate and, separately, for intraslab seismic events. We evaluated the influence of the predictive correlation models on the results corresponding to two earthquake engineering applications. The first refers to compute conditional mean spectra and the second to perform probabilistic seismic hazard analysis (PSHA) using I_{Np} and, alternatively, Sa_{avg} , intensity measures. We found that while the conditional mean spectra might be affected in the region of short vibration periods, the computations of the PSHA with improved intensity measures are not affected significantly.

KEYWORDS

conditional mean spectrum, interplate and intraslab earthquakes, PSHA, spectral correlation coefficients

1 | INTRODUCTION

The correlation coefficients are useful to define the joint distribution of spectral acceleration values at multiple periods, which allow performing different engineering applications. For instance, applications like vector-valued probabilistic seismic hazard analysis,¹ simulation of response spectra given an earthquake scenario,² and custom ground-motion prediction equations (GMPEs)^{3,4} are possible; also it is possible to perform probabilistic seismic hazard analysis (PSHA) with improved scalar intensity measures (IMs)⁵ or to construct of conditional mean spectra.^{5,6}

In this sense, Inoue and Cornell⁷ proposed an equation to predict the correlation between spectral velocity values at different vibration periods to quantify structural damage in systems of multiple degrees of freedom systems. Moreover, Cordova et al.⁸ presented a methodology to evaluate the seismic collapse performance of frame structures. This methodology includes an IM that combines the spectral acceleration measured at the fundamental period of a structure, $S_a(T_1)$, and a parameter that tries to account for structural “softening.” Therefore, it was necessary to correlate spectral acceleration values at two periods, and they used the equation developed by Inoue and Cornell. In addition, Baker and Cornell² presented an equation for correlating spectral acceleration values at two different periods; they used a data set based on worldwide recordings of shallow crustal earthquakes. Furthermore, Baker and Jayaram,⁹ using the GMPEs derived from the Next Generation Attenuation project (NGA), presented a new correlation model to predict the correlation between spectral accelerations at two vibration periods. On the other hand, Jayaram and Baker¹⁰ investigated if their correlation model⁹ predicts the correlation coefficients obtained with a Japanese ground-motion database; they observed differences in the expected correlation values, attributing them to the dependence of the characteristics of the earthquake type rather than magnitude or source-to-site distance.¹¹ Additionally, Daneshvar et al.¹² computed the correlation coefficients for Eastern Canada; they showed that correlation coefficients depend on the magnitude, and the distance-dependency is less significant. Also, they found higher correlation values than those predicted by a correlation model derived using crustal ground motions from Western North America. Therefore, selecting expressions established from seismic source areas with a particular type of rupture may not apply to other seismic regions. For example, Cimellaro¹³ used a European ground-motion database to adapt two correlation models available in the literature.^{2,14} He found that these models do not adequately predict the correlation values for that particular area. However, Ji et al.¹⁵ estimated the correlation coefficients using a Chinese ground motion database, and they found that the Baker and Jayaram model predicts with good approximation the observed results. Indeed, they used this correlation model⁹ for computing the conditional mean spectra of different sites in China.¹⁶ Additionally, the correlation between ground motion parameters has been extended at two different sites.¹⁷

In the case of Mexico, Hong and Goda¹⁸ used a ground-motion data set recorded at the central and southern zones of Mexico, and they proposed a simple correlation model for rock sites classified as B sites according to the Building Seismic Safety Council, 2004 (NEHRP). They suggest that the correlation coefficients depend on the vibration period and type of earthquake. Recently, Jaimes and Candia¹⁹ adapted the functional form proposed by Baker and Jayaram⁹ for interplate events focused on the same area and ground-motion database used in Hong and Goda.¹⁸ The advantage of this correlation model is a better prediction of correlation coefficients for vibration periods widely spaced between them. Traditionally, Mexican engineering focuses on addressing the structural and seismic engineering problems for the central and southern zones of the country. The reason is that these zones are most likely to be affected by interplate and intraslab events. The problem is in general severe for Mexico City, which due to its high-density population, particular wave propagation, and site effects makes it susceptible to earthquake damage.^{20–22}

The objective of the present study is to estimate, at firm soil site of Mexico City, the correlation coefficients between spectral acceleration values at different periods for interplate and, separately, intraslab earthquakes for comparing them with the correlations estimated from existing models available in the literature. Finally, the influence of the selected correlation models on the results obtained from two earthquake engineering applications is evaluated. The first application consists of constructing the conditional mean spectrum and the second one related to performing PSHAs using two advanced intensity measures. The first IM is the scalar intensity measure I_{Np} proposed by Bojórquez and Iervolino.^{23,24} This IM is based on $S_a(T_1)$ and a parameter proxy of the spectral shape called Np . Notice that the purpose of I_{Np} is to correct the inconveniences of traditional IMs (e.g., efficiency and sufficiency).^{25–28} The second IM is the averaged spectral acceleration $S_{a,avg}$, which is the geometric mean of spectral acceleration values over a period range. This IM may be suitable to predict the response of structures affected by excitation at different periods.⁹ Some studies compared the efficiency and sufficiency of $S_{a,avg}$ against those of $S_a(T_1)$ and showed a better prediction of the structural response when using $S_{a,avg}$.^{4,29,30} To the authors' knowledge, there is no published work that strictly addresses the applicability and the influence of different correlation models on these earthquake engineering applications.

In order to reach the objectives of the present work, as a first step, we compile interplate and intraslab ground motions recorded at the accelerometer station of Ciudad Universitaria (CU), which is within the hill zone area (firm ground) of Mexico City. Then, we select suitable GMPEs according to the conditions of the recordings. In the second step, we measure the correlations coefficients from the differences between a real response spectrum and a calculated one using its corresponding GMPE for interplate and, separately, intraslab earthquakes. In the third step, we compare our results with four predictive correlation models proposed for different seismic environments. In the fourth step,

based on hypothesis test, we propose correlation equations for Mexico City. Finally, two engineering applications are shown.

2 | FIRST STEP: ACCELEROMETER DATA AND GROUND MOTION PREDICTION EQUATIONS

Interplate and intraslab ground-motion records were compiled to perform the subsequent analyses. All the compiled ground motions are obtained only from the CU accelerometer station (firm ground). The Strong Motion Network of the Institute of Engineering at UNAM, Mexico (RAII-UNAM), provided the selected records (see Tables 1 and 2); all the records had a linear baseline correction and bandpass filter with corner frequencies of 0.1 and 25 Hz. Additionally, Figure 1 shows the epicenters of the events used in the present study.

Following, the correlation coefficients are obtained from residuals of spectral acceleration between a real response spectrum and a calculated one, using its corresponding attenuation function. Accordingly, ground motion models must

TABLE 1 Interplate seismic events recorded in CU station

Date	M_w	Distance (km)	Depth (km)	Date	M_w	Distance (km)	Depth (km)
23/08/1965	7.8	466	16	15/05/1993	6.0	320	20
02/08/1968	7.4	326	33	24/10/1993	6.7	310	19
19/03/1978	6.4	285	16	14/09/1995	7.3	320	22
29/11/1978	7.8	414	19	09/10/1995	8.0	530	27
14/03/1979	7.6	287	20	15/07/1996	6.6	301	20
25/10/1981	7.3	330	20	19/07/1997	6.7	394	15
07/06/1982	6.9	304	15	03/02/1998	6.3	509	33
07/06/1982	7.0	303	15	09/08/2000	6.5	380	33
19/09/1985	8.1	295	15	22/01/2003	7.5	526	26
21/09/1985	7.6	318	15	01/01/2004	6.0	323	15
30/04/1986	7.0	409	16	20/03/2012	7.4	329	16
25/04/1989	6.9	290	19	18/04/2014	7.2	304	10
31/05/1990	6.1	304	21				

TABLE 2 Intraslab seismic events recorded in CU station

Date	M_w	Distance (km)	Depth (km)	Date	M_w	Distance (km)	Depth (km)
06/07/1964	7.3	217	55	30/09/1999	7.4	415	47
07/06/1976	6.4	310	57	21/07/2000	5.9	146	50
24/10/1980	7.0	169	70	20/02/2006	5.2	191	56
05/08/1993	5.2	237	54	11/08/2006	6.0	228	58
23/02/1994	5.8	278	75	13/04/2007	6.0	244	43
23/05/1994	6.2	209	50	28/04/2008	5.8	195	56
10/12/1994	6.4	300	50	22/05/2009	5.6	168	59
11/01/1997	7.1	377	40	11/12/2011	6.5	176	55
03/04/1997	5.2	154	52	16/06/2013	5.9	103	52
22/05/1997	6.5	300	54	29/07/2014	6.4	432	110
20/04/1998	5.9	246	64	20/03/2015	5.4	178	61
15/06/1999	6.9	218	61	08/05/2017	7.1	105	57
21/06/1999	6.3	310	53				

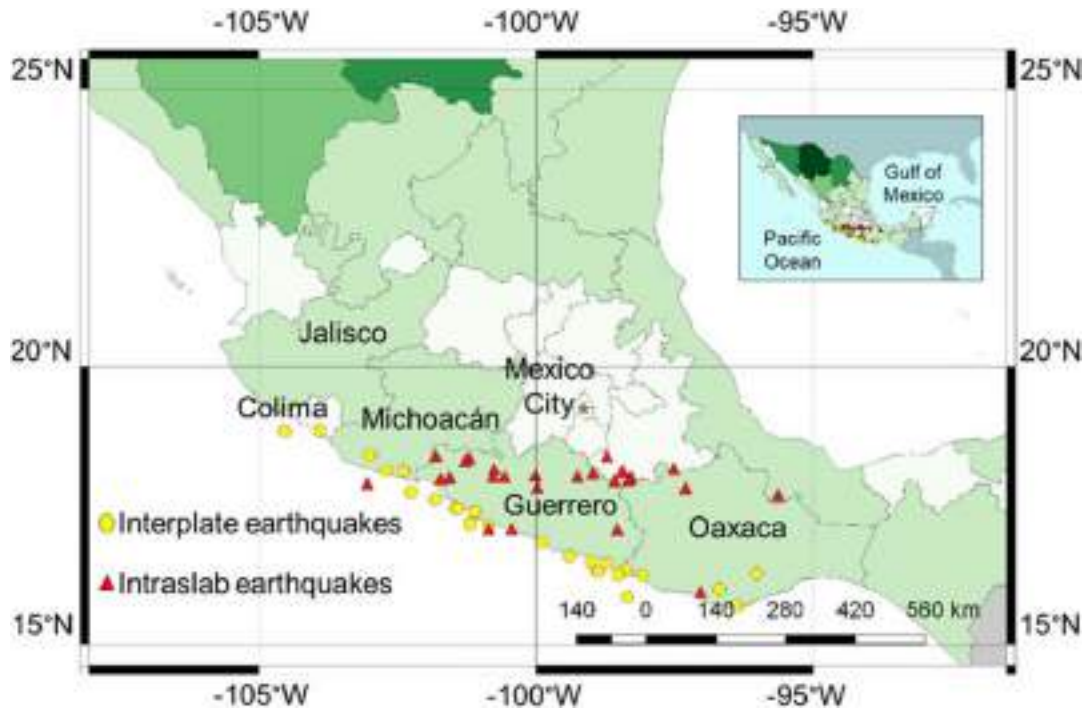


FIGURE 1 Map of southern of Mexico showing epicenters of interplate (circles) and intraslab earthquakes (triangles) used in this study [Colour figure can be viewed at wileyonlinelibrary.com]

describe a specific earthquake rupture mechanism (e.g., reverse or normal faults); otherwise, correlation coefficients may be unsuitable. Here we employ the GMPEs proposed by Reyes et al.³¹ and Jaimes et al.³² for interplate events and those proposed by Jaimes et al.³³ and García et al.³⁴ for intraslab events (hereafter denoted as Reyes02, Jaimes06, Jaimes15, and Garcia05, respectively). The interplate attenuation models resulted from the comparison between available methods to predict response spectra. They were developed using exclusively accelerometric data from CU station. Similarly, for intraslab events, Jaimes15 employed solely ground motions recorded at CU station. Meanwhile, Garcia05 employed ground motions recorded in the central and southern zones of Mexico. These attenuation models are appropriate to predict response spectra for intraslab events at sites within the hill zone of Mexico City and southern zones of Mexico, respectively.

3 | SECOND STEP: CORRELATION COEFFICIENTS BETWEEN SPECTRAL ACCELERATIONS

In order to describe the correlations adequately, it is convenient to establish that an attenuation function has the following form:

$$\ln Sa(T) = \mu_{\ln Sa}(M, R, \theta, T) + \sigma_{\ln Sa}(T) \varepsilon(T) \quad (1)$$

where $\mu_{\ln Sa}(M, R, \theta, T)$ and $\sigma_{\ln Sa}(T)$ are the predicted mean and the standard deviation of the natural logarithm of the spectral acceleration at a specified period (T), given by the attenuation model, as a function of earthquake magnitude (M), source-to-site distance (R), and other parameters (θ). Rearranging Equation 1 for $\varepsilon(T)$, it follows

$$\varepsilon(T) = \frac{\ln Sa(T) - \mu_{\ln Sa}(M, R, \theta, T)}{\sigma_{\ln Sa}(T)} \quad (2)$$

where $\varepsilon(T)$ represents the number of standard deviations by which the actual logarithmic spectral acceleration differs from the predicted mean value $\mu_{\ln Sa}(M, R, \theta, T)$ and the $\varepsilon(T)$ values at different periods are probabilistically correlated.

Additionally, the common assumption is that the residuals (epsilons) are normally distributed^{3,33,35,36}; although a study conducted by Liu et al.³⁷ suggest that the use of the whole set of intraslab ground motions (Table 2) may produce a non-normal distribution for the residuals. In this research, the $\varepsilon(T)$ values are assumed to be normally distributed for both interplate and intraslab earthquakes. Thus, the Pearson product-moment correlation coefficient is employed to measure the correlation coefficients between ε values at two natural periods $\varepsilon(T_1)$ and $\varepsilon(T_2)$, as follows:

$$\rho_{\varepsilon(T_1),\varepsilon(T_2)} = \frac{\sum_{i=1}^n (\varepsilon_i(T_1) - \varepsilon(\bar{T}_1)) (\varepsilon_i(T_2) - \varepsilon(\bar{T}_2))}{\sqrt{\sum_{i=1}^n (\varepsilon_i(T_1) - \varepsilon(\bar{T}_1))^2 \sum_{i=1}^n (\varepsilon_i(T_2) - \varepsilon(\bar{T}_2))^2}} \quad (3)$$

where $\varepsilon_i(T_1)$ and $\varepsilon_i(T_2)$ indicate the residual values evaluated for the i th ground motion record at the natural vibration periods T_1 and T_2 . The bar overhead, for $\varepsilon(T_1)$ and $\varepsilon(T_2)$, denotes the sample means of the residuals for the n number of ground motion records. The calculation is repeated for each period pair of interest. Accordingly, Figure 2 shows the correlation coefficients for a selected set of periods T_2 , plotted versus T_1 values between 0.05 and 5.0 s computed with Equation 3 (solid line). Before additional computations, we smoothed the correlation matrices estimated with Equation 3 by applying a simple averaging to the correlation coefficients associated with a subset of adjacent periods. The purpose is to establish a more manageable trend and smooth abrupt peaks or valleys of these values and eventually benefit the development of the predictive correlation equations. Thus, Figure 2 displays the effect of averaging the correlation coefficients of contiguous periods (dashed line). Finally, the smoothed correlation coefficients are employed in the present study to develop the predictive equations, assuming that these values were obtained if a broader database were available (such as those databases used in other investigations made up of hundreds of ground motions records). In the

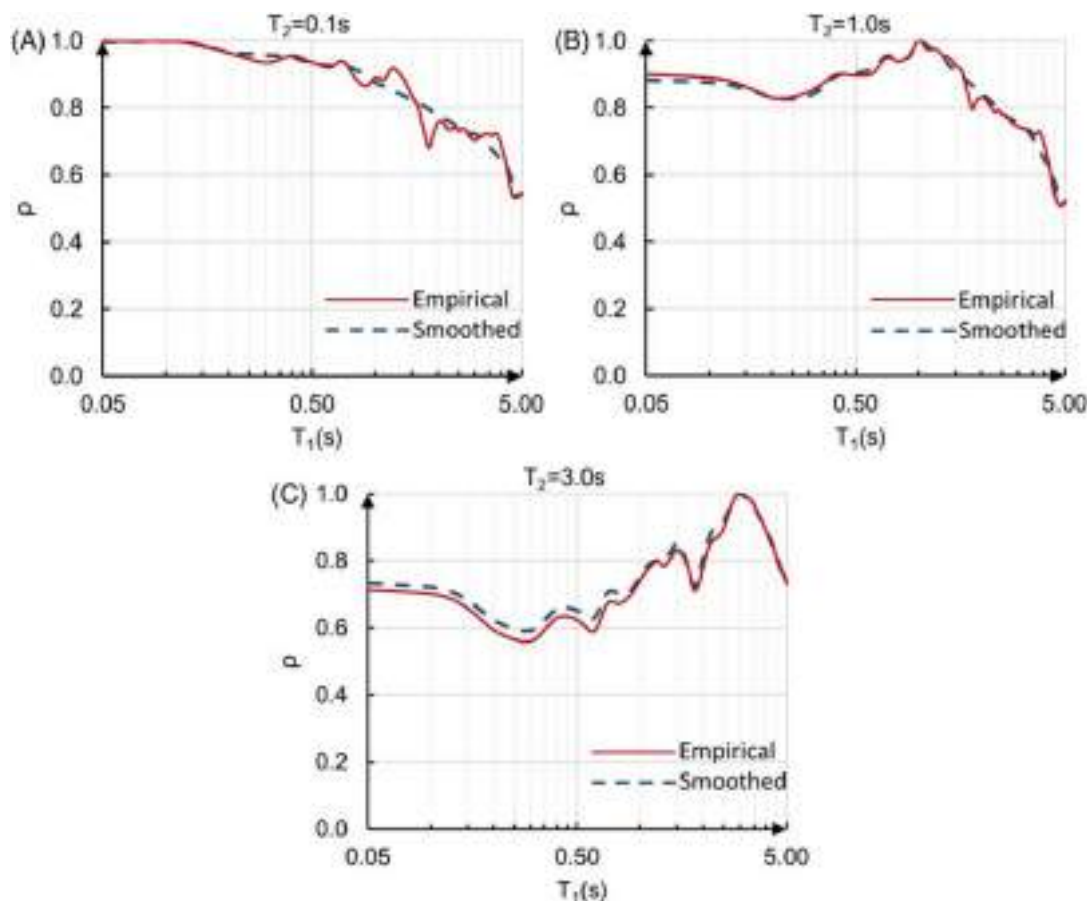


FIGURE 2 Plots of correlation coefficients versus T_1 for several T_2 values [Colour figure can be viewed at wileyonlinelibrary.com]

future, the ground motion database in Mexico City will be more extensive, and the mathematical models derived will be more precise. Therefore, it will be possible to verify models like the one proposed here.

3.1 | Correlation coefficients in CU station corresponding to *interplate* events

Figure 3A,B shows, for a selected period pairs, the correlation coefficients estimated with the *interplate* GMPEs corresponding to Reyes02 and Jaimes06, respectively. Despite Jaimes06 derived their attenuation model using only a single ground motion component, the resulting leads to similar correlations values for both GMPEs Reyes02 and Jaimes06. It is because regression analyses produce similar GMPEs independently of the definition given to the spectral acceleration.^{9,38} On the other hand, Figure 4A,B presents the same results, using contour plots of the computed correlation coefficients as a function of both T_1 and T_2 . The correlation values are between 0.4 and 1.0, and they are generally high when the separation between periods is small, although high correlation values are observed even for period pairs considerably separated. For example, the correlation associated with the period pair $\rho[\varepsilon(T_1 = 0.1 \text{ s}), \varepsilon(T_2 = 1.0 \text{ s})]$ is equal to 0.88. In this sense, Hong and Goda¹⁸ examined the correlation of spectral accelerations along the principal

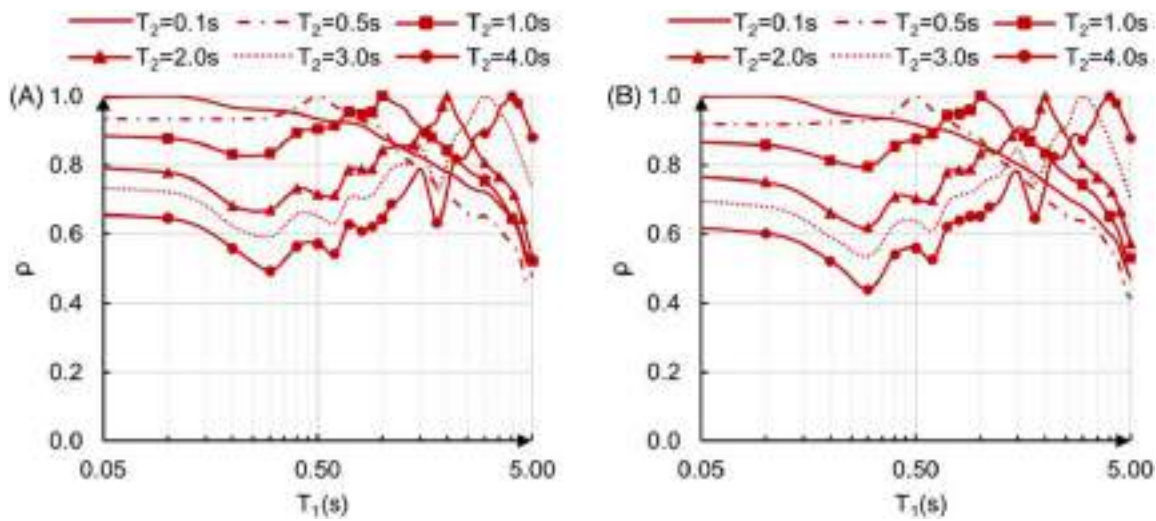


FIGURE 3 Correlation coefficients between T_1 and several T_2 values. (A) Reyes02 and (B) Jaimes06 GMPEs [Colour figure can be viewed at wileyonlinelibrary.com]

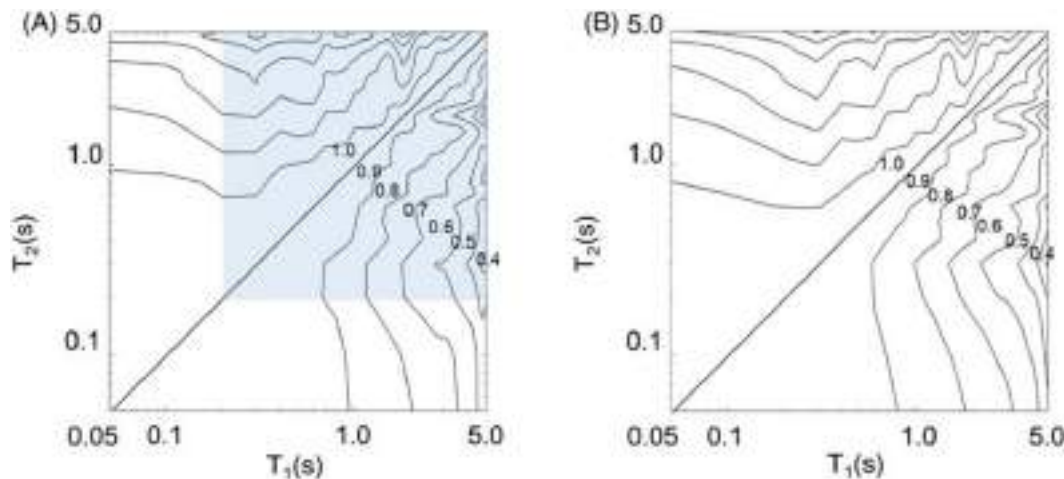


FIGURE 4 Contours of correlation coefficients between T_1 and T_2 . (A) Reyes02 and (B) Jaimes06 GMPEs [Colour figure can be viewed at wileyonlinelibrary.com]

directions of ground motions (interplate events) recorded at sites along the coast of Mexico. They found that the correlation values remained high even for well-separated vibration periods. Finally, in the present study, the comparison of the correlation values is based on the Reyes02 attenuation model, because the GMPE reports the attenuation coefficients to predict the quadratic mean of spectral acceleration values.

3.2 | Correlation coefficients in CU station corresponding to *intraslab* events

Similarly, Figures 5 and 6 show the correlation coefficients estimated using *intraslab* seismic events. First, a different spreading of correlation coefficients for intraslab events regarding interplate events stands out. Therefore, the earthquake rupture mechanism has a significant impact on the spreading of correlations. Accordingly, Jayaram and Baker¹⁰ also pointed this out using Japanese ground motions. They evaluated the correlation variation between ground motions having different earthquake rupture mechanisms, alternative tectonic sources, site conditions, ground motion models, and source-to-site distances. Finally, they concluded that correlation values appear to be dependent on the faulting type. On the other hand, the results differ significantly between the attenuation models: when using Jaimes15 model (Figure 6A), correlation values are between 0.4 and 1.0; meanwhile, with Garcia05 model (Figure 6B), the correlation

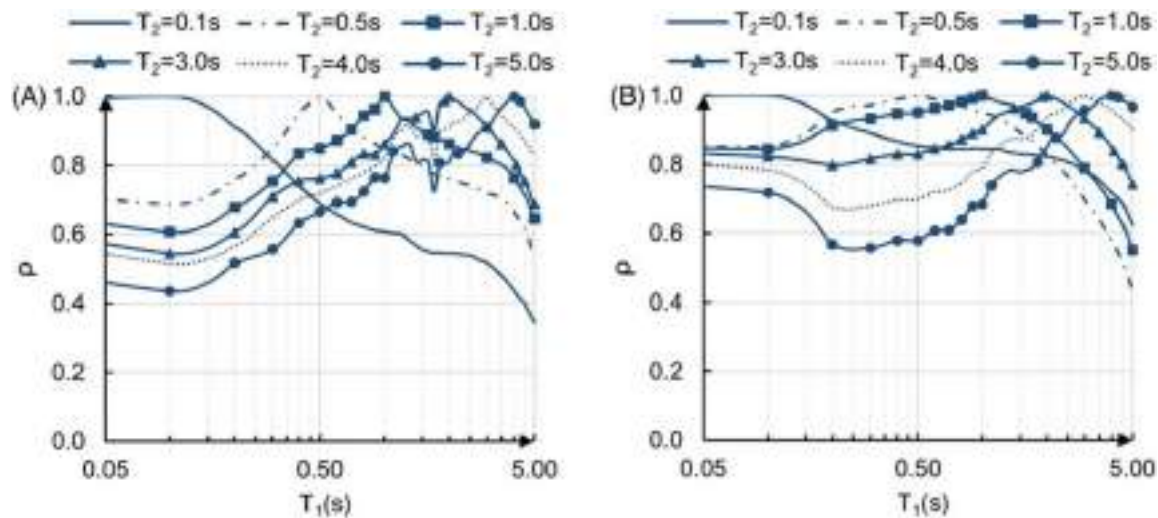


FIGURE 5 Correlation coefficients between T_1 and several T_2 values. (A) Jaimes15 and (B) Garcia05 GMPEs [Colour figure can be viewed at [wileyonlinelibrary.com](https://onlinelibrary.wiley.com)]

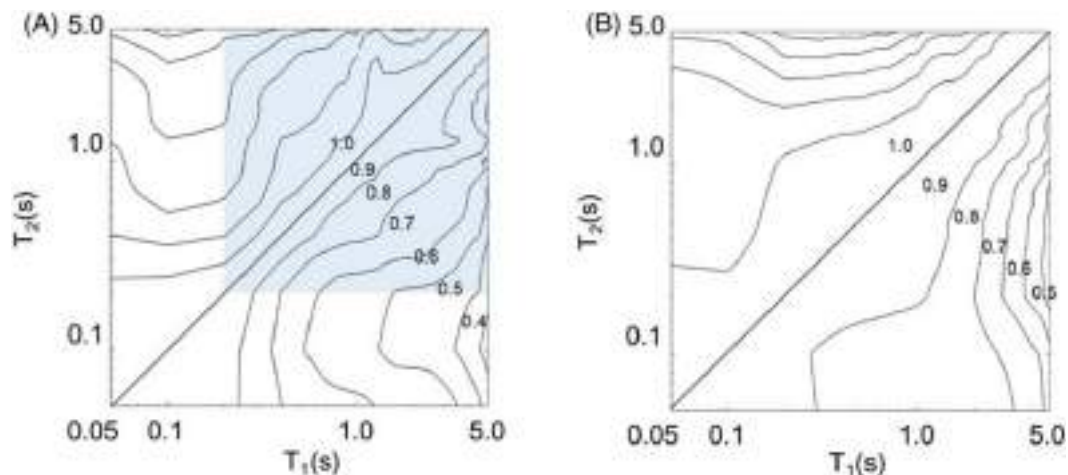


FIGURE 6 Contours of correlation coefficients between T_1 and T_2 . (A) Jaimes15 and (B) Garcia05 GMPEs [Colour figure can be viewed at [wileyonlinelibrary.com](https://onlinelibrary.wiley.com)]

remains high, between 1.0 and 0.7, for most of the period pairs. The difference is due to the following: while the first attenuation model arose of using ground motions recorded exclusively at CU station, the second one resulted from employing ground motions recorded in the central and southern zones of Mexico. Nevertheless, the Garcia05 model is included here because it has become an obligatory reference regarding seismicity associated with intraslab events in Mexico. Moreover, the Manual of Civil Structures of the Federal Commission of Electricity (CFE) suggests it as a suitable GMPE to perform probabilistic seismic hazard analysis in Mexico.³⁹ In the present study, we use the Jaimes15 attenuation model for comparison purposes presented below, therefore focusing on this attenuation model. It is observed that the correlation coefficients corresponding to pair of periods considerably spaced between them are not as high as for interplate events; however, it remains significant, for example, $\rho[\varepsilon(T_1 = 0.1 \text{ s}), \varepsilon(T_2 = 1.0 \text{ s})] = 0.63$.

4 | THIRD STEP: OBSERVED CORRELATIONS COMPARED WITH EXISTING CORRELATION MODELS

In recent years, researching regarding estimation of correlation coefficients have emerged for different seismic environments, with different purposes, for instance, PSHA with advanced intensity measures or ground motion selection. There are available models in the literature focused on predicting these correlations, for example, the well-known correlation model proposed by Baker and Jayaram.⁹ This model arose from regression analyses using a specific database (crustal earthquakes) and specific GMPEs (NGA attenuation models) and is commonly used to compare the correlation coefficients obtained from diverse seismic zones around the world.^{10,12,15} The model does an excellent job for what it was developed for; however, could it be able of describing the correlations estimated from different seismic zones and in particular for Mexico City? In order to answer this question, we compare the applicability of this model and three additional ones, for predicting the observed data from the present study (Figures 4A and 6A). The compared correlation models used in this study are those proposed by Baker and Cornell,² Baker and Jayaram,⁹ Hong and Goda,¹⁸ and Jaimes and Candia,¹⁹ hereafter referred as BC06, BJ08, HG10, and JC19, respectively. In this regard, Figure 7A–D illustrates the contour plots of correlation coefficients as a function of the vibration periods T_1 and T_2 . Additionally, there is a shaded region in each contour plot, which is also in Figures 4A and 6A; this region covers a range of periods between 0.2 and 5.0 s, and it serves as a reference for some subjects treated below.

In first place, focusing on BC06 and BJ08 models (Figure 7A,B), they were developed for Western North America to predict the correlation coefficients for shallow crustal earthquakes. These models estimate correlation values that approach to 1.0 when the pair of periods is close to one another and conversely when the periods are widely spaced between them. The latter is the general tendency when computing these correlation coefficients. For the shaded area, while BC06 and BJ08 models predict correlation values between 0.1 and 1.0, our observed correlations are between 0.4 and 1.0 for both earthquake mechanisms interplate and intraslab (see Figures 4A and 6A). However, the BC06 and BJ08 models show the spreading of correlation values represented by straight lines with a specific slope, which is similar to our observed data. Outside the shaded region, the models show that tendency of high correlation values even for pair of periods well-separated between them (as that mentioned in Section 3). This tendency becomes more significant when one of the vibration periods is short. Nevertheless, this trend is not as significant as the estimated for the firm ground of Mexico City (Figures 4A and 6A). In this regard, Carlton and Abrahamson⁴⁰ explain how for hard-rock sites with increased high-frequency content with a given dominant ground-motion period T_p , the correlation between T_p and shorter periods than this one is high. Moreover, this correlation remains high even for larger periods than T_p . This behavior is visible in the contour plots as a widening of the contour lines at short periods, which is more considerable for interplate events (see Figure 4A,B).

On the other hand, the HG10 and JC19 models (Figure 7C,D) were determined for the central and southern zones of Mexico for interplate events. The two models are based on the database compiled by Garcia et al.³⁴ and Garcia et al.⁴¹ for rock sites classified as B sites according to the NEHRP. Therefore, it is expected that these models predict similar correlation coefficients. The HG10 model predicts nearly identical values to the JC19 model for the range of periods that it was developed for. However, the JC19 model can estimate that increasing tendency of correlation values for pair of periods broadly spaced when one of these is less than 0.3 s. Then, in comparison with the observed data for the shaded region (Figures 4A and 6A), these models suitably predict the whole range of correlation values and follow a similar spreading of correlations, particularly for intraslab earthquakes. Outside this region, these models estimate inaccurate correlation values. Moreover, although the JC19 model captures the tendency of high correlation values at short periods, this tendency poorly represents the observed one, particularly for interplate events (Figure 4A,B). The

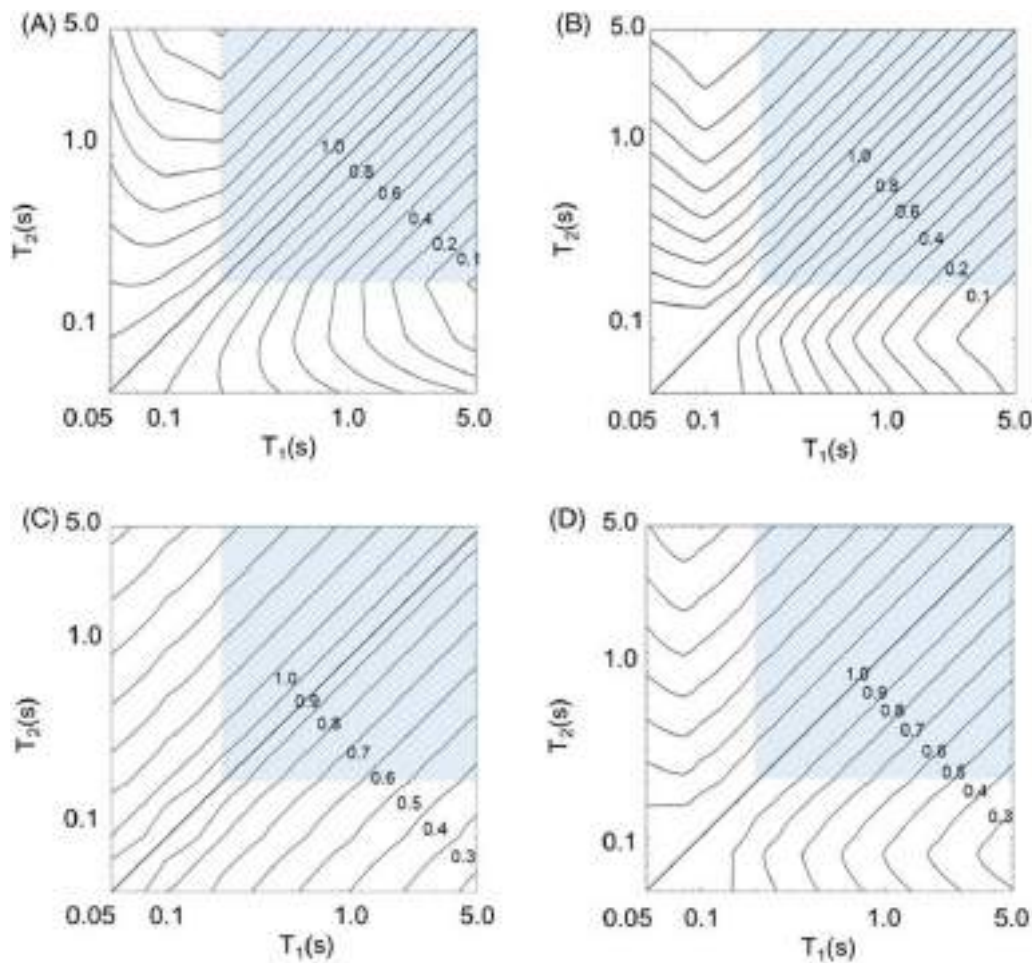


FIGURE 7 Contours of correlation coefficients between T_1 and T_2 . (A) BC06 and (B) CJ08 models and (C) HG10 and (D) JC19 models [Colour figure can be viewed at [wileyonlinelibrary.com](https://onlinelibrary.wiley.com)]

latter indicates that the sites considered by the HG10 and JC19 models are not equivalent to the sites on firm ground of Mexico City.

Summarizing, in the shaded region, the observed correlations and the analyzed correlation models describe a similar spreading of correlation values. As expected, in comparison with our results (Figures 4A and 6A), the HG10 and JC19 models predict correlation values more precise than BC06 and BJ08 models. The latter suggests that in a range of periods between 0.3 and 5.0 s, the HG10 and JC19 models estimate correlation values suitable for firm ground of Mexico City, particularly for intraslab earthquakes. Outside the shaded region, the four correlation models weakly predict the spreading of correlations observed for interplate events.

The observations above are validated with hypothesis test analyses for each period pair (T_1 , T_2), assuming H_0 , $\rho_{CU} = \rho_{existing\ models}$, and H_1 , $\rho_{CU} \neq \rho_{existing\ models}$, as the null and alternative hypothesis, respectively, with a significance level of $\alpha_0 = 5\%$ (see Figure 8). For all the analyzed correlation models concerning interplate earthquakes, the analyses confirm that the correlation coefficients estimated with existing models can be accepted when the pair of periods are both relatively high (see dark zone of Figure 8A). However, they cannot be accepted when the periods are broadly spaced, mostly when one of these is short (see bright zone of Figure 8A). On the other hand, regarding intraslab earthquakes, the acceptance depends on the model used for the analysis. Figure 8B shows that the correlation coefficients, estimated with models that were no developed employing Mexican records, cannot be accepted for a wide region of period pairs. Nevertheless, the correlations computed with models developed using Mexican records (e.g., HG10 and JC19) have a better performance (see Figure 8C). From these results, we can infer that the use of any of the analyzed models for predicting spectral correlations associated with interplate earthquakes might affect to short periods of the engineering applications presented below. On the other hand, we consider in advance that to estimate the spectral

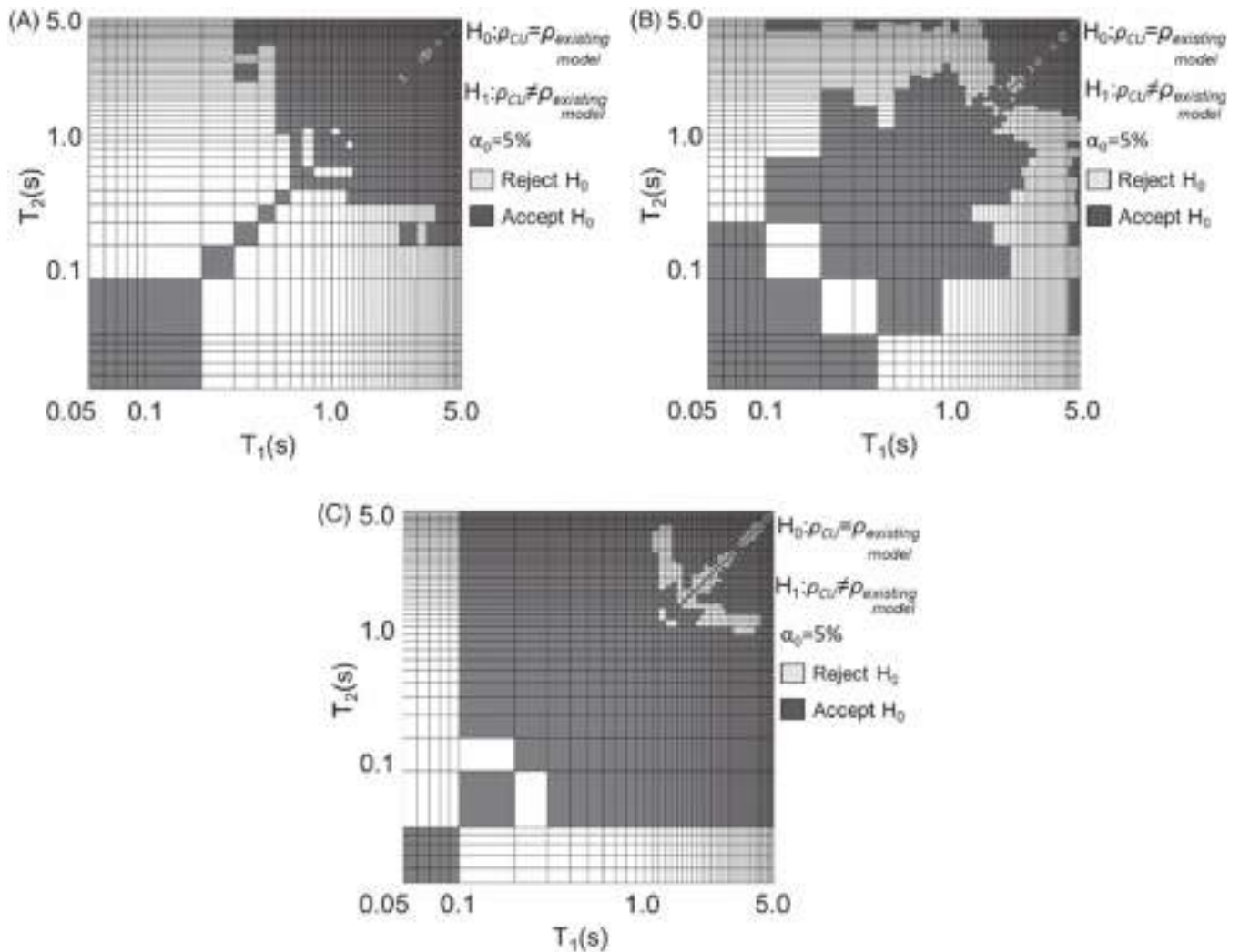


FIGURE 8 Hypothesis test tendency for each period pair (T_1 , T_2) when using (A) all the models and interplate earthquakes, (B) BC06 and BJ08 models and intraslab earthquakes, and (C) HG10 and JC19 models and intraslab earthquakes

correlations with the HG10 and JC19 models, related to intraslab earthquakes, might have a minor influence on the engineering applications. Therefore, based on the above analyses, a predictive correlation equation is proposed.

5 | FOURTH STEP: PREDICTIVE CORRELATION MODEL FOR FIRM GROUND IN MEXICO CITY

The estimated correlation coefficients from Section 3 can be used when they are needed; however, it would be troublesome due to the dimension of each correlation matrix. Therefore, a mathematical expression is fitted to the observed data (Figures 4A and 6A). Moreover, the proposed correlation model will be a comparing point regarding the obtained results from the engineering applications when employing the analyzed correlation models. Accordingly, the proposed model must predict accurate correlation values for period pairs when one of these is short, which is what is lacking in the four analyzed models. Also, we keep the model as simple as possible with a unique functional form for both earthquake rupture mechanisms. Nonlinear least-squares regression is applied to find the associated parameters for the equation. The nonlinear performance of the least-squares method is better when the errors for each observed value are of comparable size⁹; however, this is not the case. The computed correlation coefficients have no constant standard errors, and the variance of the correlation coefficients ρ usually becomes smaller when it approaches 1 or -1 . Therefore, the Fisher z transformation is employed, which transforms the correlation coefficients into a normally distributed

variable z (see Equations 4 and 5). Additionally, the standard error of z becomes a known constant, depending solely on the sample size n .⁴²

$$z = \frac{1}{2} \ln \left(\frac{1 + \rho}{1 - \rho} \right) \quad (4)$$

$$\text{std}(z) = \frac{1}{\sqrt{n-3}} \quad (5)$$

where ρ is the correlation coefficient computed with Equation 3 and z is the transformed variable. Then, the nonlinear least-squares method is applied to the modified values, rather than to the original correlation values estimated with the equation mentioned above, via

$$\min_{\beta} \sum_{i=1}^n \sum_{j=1}^n \left(\frac{1}{2} \ln \left(\frac{1 + \rho_{ij}}{1 - \rho_{ij}} \right) - \frac{1}{2} \ln \left(\frac{1 + \tilde{\rho}_{ij}(\beta)}{1 - \tilde{\rho}_{ij}(\beta)} \right) \right) \quad (6)$$

where ρ_{ij} is the correlation coefficient at the period pair (T_i, T_j) and $\tilde{\rho}_{ij}(\beta)$ is the predicted correlation using the proposed predictive equation with a vector of parameters β associated with that mathematical expression.

5.1 | Predictive correlation model for *interplate* and *intraslab* events

The predictive correlation equation proposed here is the following:

$$\rho \ln[Sa(T_i)], \ln[Sa(T_j)] = \frac{a + bT_{\min} + cT_{\max}}{1 + dT_{\min} + eT_{\max}} - f \ln \left(\frac{T_{\max}}{T_{\min}} \right) \quad (7)$$

where $T_{\min} = \min(T_1, T_2)$ and $T_{\max} = \max(T_1, T_2)$; the numerical coefficients $a, b, c, d, e,$ and f are in Tables 3 and 4 for interplate and intraslab events, respectively.

Figure 9A,B shows the correlation coefficients for a selected set of periods T_2 , plotted versus T_1 values between 0.05 and 5.0 s, for interplate and intraslab events, respectively. Meanwhile, Figure 10A,B shows the corresponding contours of correlation coefficients between T_1 and T_2 for interplate and intraslab seismic events, respectively. In this study, the predicted correlation corresponds to the quadratic mean of spectral accelerations at two vibration periods. Finally,

TABLE 3 Numerical coefficients for interplate predictive correlation equation

Restriction	a	b	c	d	e	f
$T_{\min} \leq 0.3$	1.244	-0.704	-0.1415	0.52	-0.092	0.081
$T_{\min} \geq 0.2$	0.991	0.432	0.0496	0.06	0.413	-0.018
$T_{\min} < 0.1$ or $T_{\min} = 0.1$ & $T_{\max} > 1.0$	1.222	3.374	-0.188	5.00	-0.139	0.059
$T_{\max} > 4.4$ & $T_{\min} \geq 0.2$ & $T_{\min} \leq 1.0$	-0.220	4.704	-4.2504	5.00	0.482	-1.586

TABLE 4 Numerical coefficients for intraslab predictive correlation equation

Restriction	a	b	c	d	e	f
	0.831	4.887	0.1499	5.00	-0.061	0.216
$T_{\min} \geq 0.3$	0.984	-0.029	-0.1624	-0.04	-0.16	0.135
$T_{\max} < 3.0$ & $T_{\min} \leq 0.2$	1.479	0.722	1.0289	3.95	0.433	0.35
$T_{\min} < 0.1$ & $T_{\max} > 1.0$	0.907	-1.859	-0.1306	-0.04	-0.14	0.00

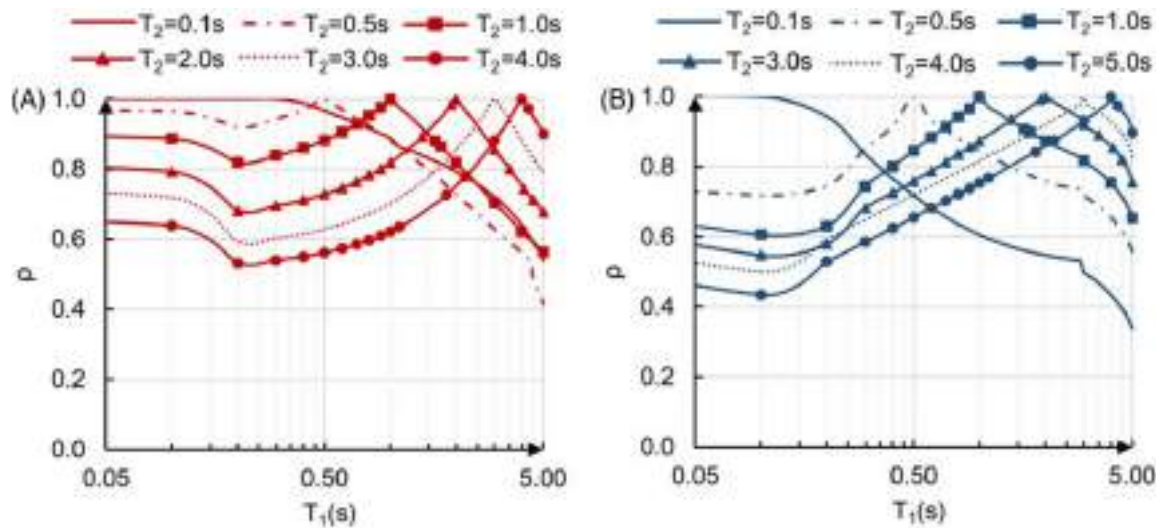


FIGURE 9 Plots of correlation coefficients versus T_1 , for several T_2 values. Using predictive correlation equations: (A) interplate and (B) intraslab [Colour figure can be viewed at wileyonlinelibrary.com]

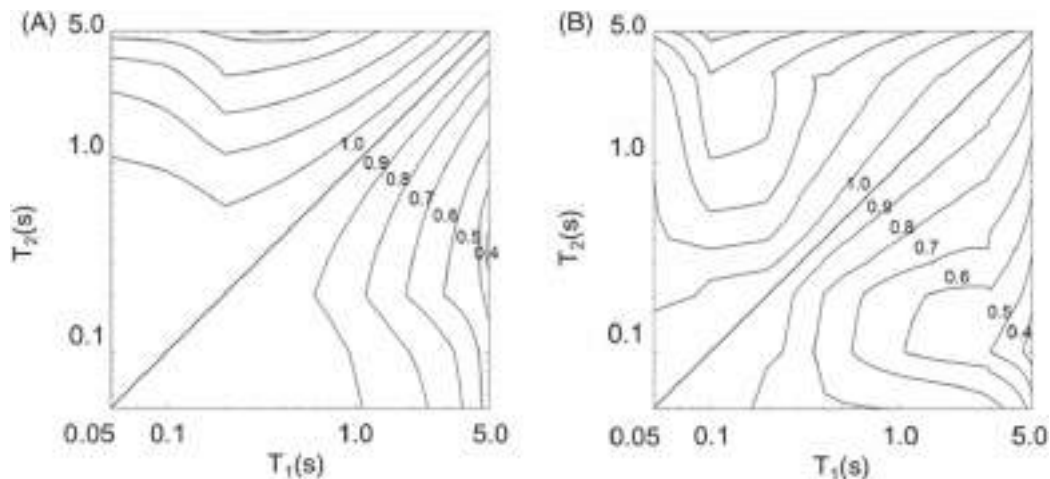


FIGURE 10 Contours of correlation coefficients between T_1 and T_2 . Using the predictive correlation equation for (A) interplate and (B) intraslab events

GMPEs are developed commonly to predict the geometric or quadratic mean of spectral acceleration values of the two horizontal components of motion. They are also established to predict the spectral acceleration corresponding to a single horizontal component. No matter the definition of the spectral acceleration that an attenuation model employs, the predicted spectral values are similar,^{9,38} which is evident in Figure 4A,B. In conclusion, the above paragraph indicates that the proposed mathematical expressions are applicable independently of the GMPEs, as suggested elsewhere.^{2,9} In this case, the proposed correlation model is useful as long as the GMPEs had been derived entirely for the firm ground of Mexico City.

6 | FIFTH STEP: TWO EARTHQUAKE ENGINEERING APPLICATIONS

In order to compare the influence of the presented correlation models on earthquake engineering applications, two applications are performed. The first one is related to computing conditional mean spectra, which we consider, in advance, that might be affected at the region of short periods, especially for interplate earthquakes; however, it remains to be confirmed; and the second one is associated with PSHA using advanced IMs.

6.1 | First engineering application: conditional mean spectrum

Selection of earthquakes ground motion records is an essential issue for the assessment of structures using nonlinear dynamic analysis. In practice, ground motion selection is generally based on selecting ground motion records that match a target spectrum, commonly, the uniform hazard spectrum; however, this spectrum is not an appropriate target spectrum because it is significantly conservative for some purposes.^{6,13,43} Accordingly, Baker and Cornell^{5,6} proposed a target spectrum useful for ground-motion selection; it considers the magnitude (M), distance (R), and ϵ values likely to cause a specific intensity level at a site. They suggest that rather than attempt to find ground-motion records that match the M , R , and ϵ values, these can be employed to estimate the conditional mean spectrum (CMS). Therefore, one could base the record selection on this type of spectrum. This approach should increase the number of acceptable records for the analysis, because ground-motion records need solely to have a spectral shape that matches that target spectrum. Additionally, using the CMS decreases the dispersion of the structural dynamic response.

To construct the target spectrum, in this application, we first select a target value of spectral acceleration, denoted as $Sa(T^*)$, corresponding to a given probability of exceedance (e.g., 10% in 50 years) at a period of interest $T^* = 1.0$ s at CU site. Then, through a PSHA deaggregation process,⁴⁴ we identify the mean magnitude (\bar{M}), distance (\bar{R}), and $\bar{\epsilon}(T^*)$ values that cause the occurrence of $Sa(T^*)$ (see Figure 11A,B).

It follows from Figure 11A that the mean values obtained correspond to an interplate earthquake; as expected, it has been recognized that PSHA is governed by interplate events for flexible systems and intraslab events for stiff systems.³⁷ Therefore, we select an appropriate GMPE to compute the mean and standard deviation of log spectral acceleration values at all periods, for the \bar{M} and \bar{R} values obtained from the deaggregation analysis. Subsequently, knowing the $\bar{\epsilon}(T^*)$ value, the conditional distribution of $Sa(T_i)$ values at other periods can be estimated as:

$$\mu_{\ln Sa(T_i)|\ln Sa(T^*)} = \mu_{\ln Sa}(M, R, \theta, T_i) + \rho_{\ln[Sa(T_i)], \ln[Sa(T^*)]} \epsilon(T^*) \sigma_{\ln Sa}(T_i) \quad (8)$$

where the means $\mu_{\ln Sa}(M, R, \theta, T)$ and the standard deviations $\sigma_{\ln Sa}(T)$ of the logarithm of the response spectral values are obtained with the interplate GMPE of Section 2. Meanwhile, the correlation coefficients $\rho_{\ln[Sa(T_i)], \ln[Sa(T^*)]}$ are predicted with Equation 7. Finally, the exponential of the $\mu_{\ln Sa(T_i)|\ln Sa(T^*)}$ values represent the conditional mean spectrum. Accordingly, Figure 11A,B shows the conditional mean spectra using the correlation model proposed in this study (solid line) together with the BJ08 and JC19 models (dashed lines), respectively. The conditional mean spectra are estimated for $Sa(T^* = 1.0)$ with different probabilities of exceedance (10%, 20%, and 40% in 50 years).

Figure 12A,B shows the conditional mean spectra using the BJ08 and JC19 models (dashed lines) and the proposed model (solid lines), respectively. They show an underestimation of the spectral values at the region of short periods when using the BJ08 and JC19 models in comparison with the proposed correlation model, which is consistent with that reported in previous sections (Section 4). The latter is because the four correlation models predict lower correlation values than those observed, predominantly, at period pairs when one of these is relatively short. Therefore, as expected, the underestimation is more significant at short vibration periods; also, it increases as the return interval grows. On

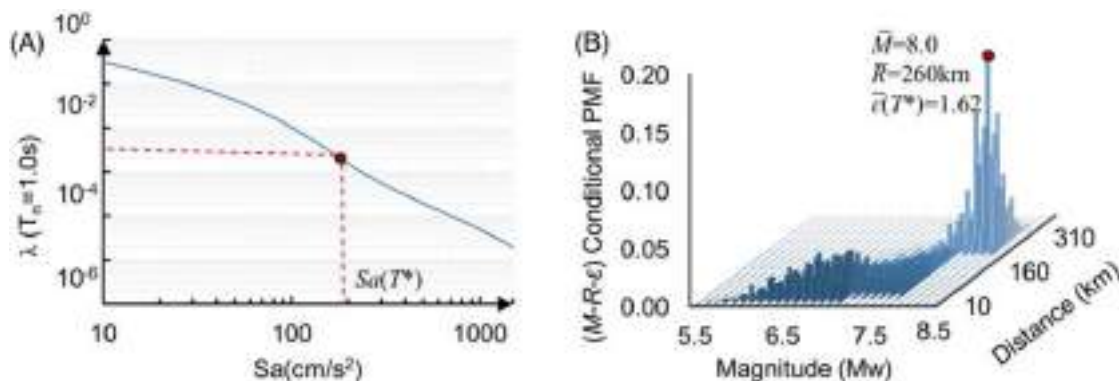


FIGURE 11 (A) $Sa(T^*)$ mean annual rate of exceedance (λ) at $T_n = 1.0$ s and (B) PSHA deaggregation for CU station, given exceedance of $Sa(T^*)$ values with 475-year return period, at $T_n = 1.0$ s [Colour figure can be viewed at wileyonlinelibrary.com]

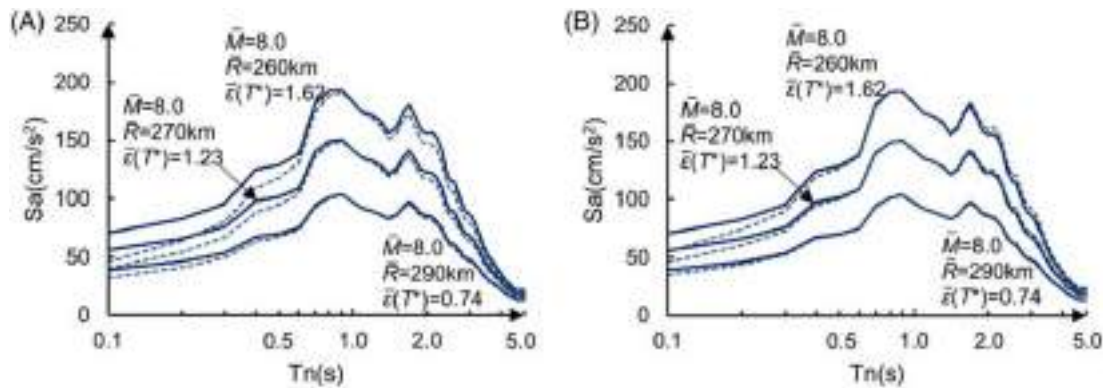


FIGURE 12 Conditional mean spectra for CU site given occurrence of $Sa(T_1 = 1.0)$ values with 10%, 20% and 40% of probability of exceedance in 50 year. (A) Using the proposed correlation model (solid line) and BJ08 correlation model (dashed line) and (B) using the proposed correlation model (solid line) and the JC19 correlation model (dashed line) [Colour figure can be viewed at [wileyonlinelibrary.com](https://onlinelibrary.wiley.com)]

the other hand, at the region of long periods, the conditional mean values are similar. The same tendency was found for the BC06 and HG10 models (not shown here).

Additionally, we perform the same analysis above, but now choosing as a period of interest $T^* = 0.2$ s. Then, through a deaggregation analysis, we identify the mean magnitude (\bar{M}) and distance (\bar{R}) values, which correspond to an intraslab event.³⁷ Therefore, according to the GMPE for intraslab events, the resulted spectra are shown below. Figure 13A,B indicates the conditional mean spectra for intraslab events estimated with the BC06 and HG10 models (dashed lines) and the proposed correlation model (solid lines), respectively. They show good agreement of the spectral values for the three correlation models at the whole range of periods. The results are the same for the BJ08 and JC19 models (not shown here). As it was pointed out in Section 3.2, high correlation values persist for intraslab events at broadly spaced period pairs; however, this increasing tendency is not as significant as it is for interplate events. Therefore, for period pairs when one of these is less than 0.2 s, the widening of the contour lines is small. Thus, the spreading of the correlation coefficients for intraslab events is comparable with that predicted by the compared correlation models. Consequently, the conditional mean values are practically identical for the four correlation models (BC06, BJ08, HG10, and JC19) compared with the proposed one, even when these models were not developed for intraslab earthquakes (Figure 13A,B). According to the hypothesis test analyses (see Figure 8C), we were expecting a suitable performance of the HG10 and JC19 models. However, the BC06 and BJ08 models have also good performance, contrary to one may expect from the hypothesis test analyses for intraslab earthquakes (see Figure 8B).

In summary, Figures 12 and 13 show that, for computing conditional mean spectra, to use one or other correlation model only influence on the region of short periods when interplate earthquakes control the deaggregation process. In

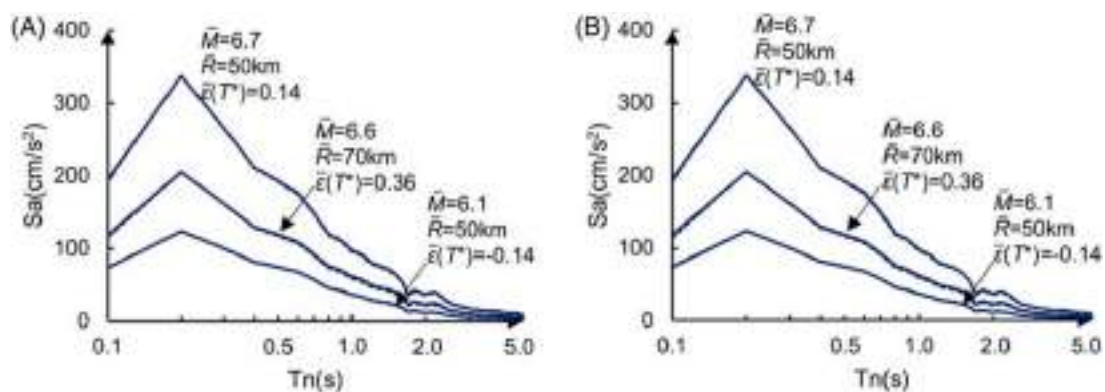


FIGURE 13 Conditional mean spectra for CU site given occurrence of $Sa(T_1 = 0.2)$ values with 10%, 20%, and 40% of probability of exceedance in 50 year. (A) Using the proposed correlation model (solid line) and BJ06 correlation model (dashed line) and (B) using the proposed correlation model (solid line) and the HG10 correlation model (dashed line) [Colour figure can be viewed at [wileyonlinelibrary.com](https://onlinelibrary.wiley.com)]

this sense, Ji et al.^{15,16} computed the CMS for two different sites in China. For this purpose, they used the correlation coefficients obtained from a Chinese ground motion database, and the correlations predicted with the BJ08 correlation model. They found that the conditional mean values obtained with the BJ08 model are lower than the spectral values obtained using their correlation coefficients. However, this discrepancy was not significant, and they suggest the BJ08 model appropriate to compute CMS in China. Additionally, Cimellaro¹³ estimated the correlation coefficients and proposed a predictive correlation model using a European database. Then, for a site in Italy, he computed the CMSs employing his correlation model and the BC06 model. The comparison between the two CMSs indicates that spectral values are practically identical over the whole period range. The latter is true even when the spreading of correlation coefficients was completely different from that obtained for shallow crustal earthquakes from California.

6.2 | Second engineering application: seismic hazard curves using two intensity measures

Following, in this example, we proceed with the PSHA, presenting the results through mean annual rates of exceedance (hazard curves), using the two intensity measures (IM) presented in the introduction of this study. The advantages of employing one or another intensity measure are not the subject on which this section focuses. The predictive correlation models are suitable to any intensity measure that acts as a function of spectral acceleration values at different vibration periods. Therefore, the reader is free to utilize the IM of his or her preference.

The application of advanced intensity measures is limited because of the lack of appropriate GMPEs, which are essential for performing PSHA. For instance, attenuation models have not yet devised, to provide I_{Np} and Sa_{avg} as a function of the vibration period, as it is done with existing GMPEs. But, fortunately, with tools currently available for other IMs and the predictive correlation models presented in this study, it is possible to define the expected value and the variance of the natural logarithm of both intensity measures I_{Np} and Sa_{avg} and finally to perform PSHA. In what follows, it is presented the development to define the expected value and the variance of the natural logarithm of I_{Np} (a similar scheme for Sa_{avg} can be found in Baker and Cornell³ and Baker and Jayaram⁹). First, I_{Np} is defined as follows²⁴:

$$I_{Np} = Sa(T_1) \cdot N_p^\alpha \quad (9)$$

$$N_p = \frac{\bar{S}a_{avg}(T_1 \dots T_N)}{Sa(T_1)} \quad (10)$$

where I_{Np} is the scalar intensity measure and α is a parameter that should be calibrated according to the structure and the earthquake demand parameter selected (in this study $\alpha = 0.5$ is adopted, as recommended in Bojórquez and Iervolino²⁴). $\bar{S}a_{avg}$ is the geometric mean of the spectral acceleration at N numbers of periods, expressed as

$$\bar{S}a_{avg}(T_1 \dots T_N) = \left(\prod_{i=1}^N Sa(T_i) \right)^{1/N} \quad (11)$$

Substituting Equations 10 and 11 in Equation 9 and applying the natural logarithm, it results

$$\ln(I_{Np}) = (1 - \alpha) \ln[Sa(T_1)] + \frac{\alpha}{N} \sum_{i=1}^N \ln[Sa(T_i)] \quad (12)$$

Then, the expected value and the variance of $\ln(I_{Np})$ can be expressed as in Equations 13 and 14, respectively.

$$E[\ln(I_{Np})] = (1 - \alpha) E\{\ln[Sa(T_1)]\} + \frac{\alpha}{N} \sum_{i=1}^N E\{\ln[Sa(T_i)]\} \quad (13)$$

$$\begin{aligned} \text{Var}[\ln(I_{Np})] &= \alpha^2 \text{Var}\{\ln[Sa_{avg}(T_1 \dots T_N)]\} + (1-\alpha)^2 \text{Var}\{\ln[Sa(T_1)]\} \\ &+ 2\alpha(1-\alpha)\rho_{\ln[Sa_{avg}(T_1 \dots T_N)], \ln[Sa(T_1)]} \sigma_{\ln[Sa_{avg}(T_1 \dots T_N)]} \sigma_{\ln[Sa(T_1)]} \end{aligned} \quad (14)$$

The $\ln[Sa(T_i)]$ values are obtained from existing attenuation models (e.g., the GMPEs presented in Section 2); $\ln[Sa(T_i)]$ terms are commonly assumed to have a joint normal distribution; consequently, the summation has also a normal distribution. The variance $\text{Var}\{\ln[Sa_{avg}(T_1 \dots T_N)]\}$ and the correlation coefficient $\rho_{\ln[Sa_{avg}(T_1 \dots T_N)], \ln[Sa(T_1)]}$ can be obtained by Equations 15 and 16, respectively:

$$\text{Var}\{\ln[Sa_{avg}(T_1 \dots T_N)]\} = \frac{1}{N^2} \sum_{i=1}^N \sum_{j=1}^N \left[\rho_{\ln[Sa(T_i)], \ln[Sa(T_j)]} \sigma_{\ln[Sa(T_i)]} \sigma_{\ln[Sa(T_j)]} \right] \quad (15)$$

$$\rho_{\ln[Sa_{avg}(T_1 \dots T_N)], \ln[Sa(T_1)]} = \frac{\sum_{i=1}^N \rho_{\ln[Sa(T_i)], \ln[Sa(T_1)]} \sigma_{\ln[Sa(T_i)]}}{\sqrt{\sum_{i=1}^N \sum_{j=1}^N \left[\rho_{\ln[Sa(T_i)], \ln[Sa(T_j)]} \sigma_{\ln[Sa(T_i)]} \sigma_{\ln[Sa(T_j)]} \right]}} \quad (16)$$

where $\rho_{\ln[Sa(T_i)], \ln[Sa(T_j)]}$ is the correlation between spectral acceleration values at periods T_i and T_j , which are computed using a correlation equation (in our case, Equation 7). Thus, a customized attenuation model for I_{Np} has been established. All these equations are enough to describe the complete distribution of I_{Np} .

Figure 14A,B illustrates the I_{Np} mean annual rate of exceedance, λ , for two vibration periods $T_1 = 0.2$ s and $T_1 = 2.0$ s, respectively. Similarly, Figure 15A,B shows the mean annual rate of exceedance of Sa_{avg} , for $T_1 = 0.2$ s and $T_1 = 2.0$ s, respectively (the range of periods for Sa_{avg} was taken from T_1 to $2T_1$, spaced each 0.1 s). The I_{Np} and Sa_{avg} hazard curves correspond to two accelerometer stations installed in Mexico City: CU and Ministry of Communications and Transportation of Mexico (SCT), as shown in Figures 14 and 15. CU station is within the hill zone area (firm ground); meanwhile, SCT station is in the lake-bed zone area (soft soil) in Mexico City. The annual rates of exceedance of the seismic intensity are estimated using the correlation model proposed in this study, along with the four correlation models mentioned above.

The I_{Np} and Sa_{avg} hazard curves for CU station are computed combining the above development and the traditional PSHA.⁴⁵ On the other hand, the hazard curves for SCT station are calculated with the formulation proposed by Esteva,⁴⁶ which allows, through a known hazard curve at a given site (reference site), to estimate a hazard curve in a different one (recipient site). It is possible by coupling this formulation with the ratio between response spectra corresponding to soft soil (recipient site) and firm ground (reference site). The spectral ratios represent, approximately, the spectral amplification in soft soil concerning firm ground. In this study, CU station is the reference site, because, since 1964, it has recorded all the significant ground motions that have struck Mexico City. Accordingly,

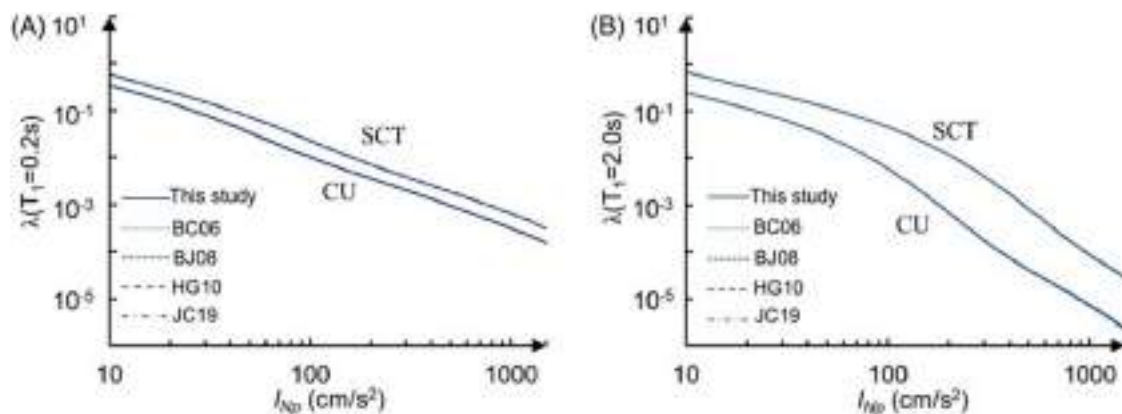


FIGURE 14 Mean annual rate of exceedance (λ) of I_{Np} for recording stations located on firm ground (CU) and soft soil (SCT) in Mexico City, for two different fundamental vibration periods, (A) $T_1 = 0.2$ s and (B) $T_1 = 2.0$ s [Colour figure can be viewed at wileyonlinelibrary.com]

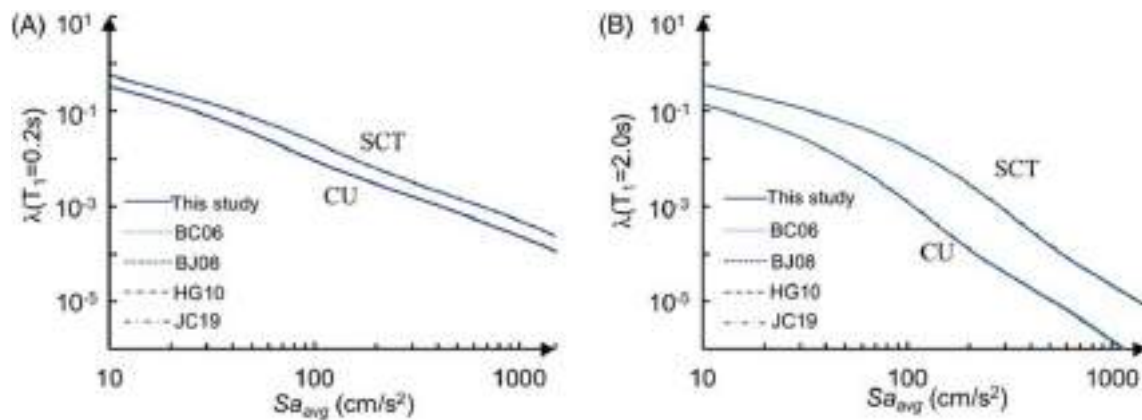


FIGURE 15 Mean annual rate of exceedance (λ) of Sa_{avg} for recording stations located on firm ground (CU) and soft soil (SCT) in Mexico City, for two different fundamental vibration periods, (A) $T_1 = 0.2$ s and (B) $T_1 = 2.0$ s [Colour figure can be viewed at wileyonlinelibrary.com]

different studies have taken CU as a reference site.^{47–49} Thus, it is feasible to perform a hazard analysis for CU station and then to compute the annual rate of exceedance at other recording stations located on soft soils in Mexico City.

It is observed that the I_{Np} and Sa_{avg} hazard curves, for each recording station, are nearly identical independently of the correlation model used. Indeed, the overlapping of the hazard curves makes us to look as there is only one hazard curve for each site. Therefore, for this engineering application, it is concluded that it is enough to have a predictive correlation model that, roughly, predicts the spreading of correlations. Thus, one can set aside the searching for a high grade of detail to match exactly the observed data.

7 | CONCLUSIONS

- We estimated the correlation coefficients between spectral accelerations values at multiple vibration periods using ground motions recorded at the CU accelerometer station (firm ground) in Mexico City. For this purpose, we utilized GMPEs to predict, exclusively, interplate or intraslab seismic events. We found a different spreading of correlations when we measured the correlation coefficients using interplate and, independently, intraslab ground motions. It shows that the correlation coefficients depend strongly on the rupture mechanism.
- We made an exhaustive comparison of different correlation models found in the literature to assess if they correctly predict our observed correlation coefficients. We observed that, mainly, at pairs of periods when one of these is shorter than 0.3–0.4 s, the presented models predict inaccurate correlation coefficients for interplate and intraslab earthquakes, which was also proven with a hypothesis test. Due to the findings, it was justified to propose a predictive correlation equation for the cases of this study.
- We proposed a mathematical expression to estimate the correlation coefficients between spectral acceleration values at multiple periods corresponding to interplate and, separately, to intraslab earthquakes, for the firm ground of Mexico City. Additionally, the proposed model addressed the shortcomings presented by the studied models for the prediction of correlation values for short periods.
- We evaluate the influence of the analyzed correlation models on the results from conditional mean spectra and PSHAs with two IMs. Consistently with the hypothesis test and the results from Section 6.1, we concluded that the conditional mean spectra are only affected at the region of short periods, specifically when interplate earthquakes govern the deaggregation process. Conversely, when intraslab earthquakes control the deaggregation process, the conditional mean values are basically the same independently of the correlation model used. On the other hand, for PSHAs using I_{Np} or Sa_{avg} , to use one or another correlation model does not affect the results significantly. It is worth noting that, even when the four correlation models analyzed predict inaccurate correlation values at specific period pairs, the latter does not have a significant impact on the results. Therefore, we concluded that the five correlation

models used for comparison (BC06, BJ08, HG10, JC19, and the one proposed here) are suitable for computations related to PSHAs associated with I_{Np} or, alternatively, with Sa_{avg} .

- For the purpose of estimating seismic hazard curves, it is recommended to focus on having an appropriate ground motion database instead of searching for an equation that predicts the correlation coefficients with a high degree of correctness, which at the same time would result in a more complex mathematical model.
- For the applications analyzed in the present study, simplified models like BC06 and HG10 lead to results with good approximation, from the point of view of earthquake engineering.

ACKNOWLEDGEMENTS

The present study is part of the projects PAPIIT IN103517 and IN100320 of DGAPA-UNAM. The authors wish to thank CIRES for having provided the seismic records used in this study. The first author wishes to thank CONACyT for the support given during his graduate studies.

ORCID

Ali Rodríguez-Castellanos  <https://orcid.org/0000-0002-2068-8194>

Sonia E. Ruiz  <https://orcid.org/0000-0002-2731-6780>

Edén Bojórquez  <https://orcid.org/0000-0001-6402-1693>

Alfredo Reyes-Salazar  <https://orcid.org/0000-0001-5074-1526>

REFERENCES

1. Bazzurro P, Cornell CA. Vector-valued probabilistic seismic hazard analysis. 7th U.S. National Conference on Earthquake Engineering. Boston, MA: Earthquake Engineering Research Institute; 2002:10.
2. Baker JW, Cornell CA. Correlation of response spectral values for multicomponent ground motions. *Bull Seismol Soc Am*. 2006;96(1):215-227. <https://doi.org/10.1785/0120050060>
3. Baker JW, Cornell CA. Spectral shape, epsilon and record selection. *Earthq Eng Struct Dyn*. 2006;35(9):1077-1095. <https://doi.org/10.1002/eqe.571>
4. Kohrangi M, Kotha SR, Bazzurro P. Ground-motion models for average spectral acceleration in a period range: direct and indirect methods. *Bull Earthq Eng*. 2018;16(1):45-65. <https://doi.org/10.1007/s10518-017-0216-5>
5. Baker JW, Cornell CA. A vector-valued ground motion intensity measure consisting of spectral acceleration and epsilon. *Earthq. Eng. Struct. Dyn*. 2005;34(10):1193-1217. <https://doi.org/10.1002/eqe.474>
6. Baker JW. Conditional mean spectrum: tool for ground-motion selection. *J Struct Eng*. 2011;137(3):322-331. [https://doi.org/10.1061/\(ASCE\)ST.1943-541X.0000215](https://doi.org/10.1061/(ASCE)ST.1943-541X.0000215)
7. Inoue T, Cornell CA. *Seismic hazard analysis of multi-degree-of-freedom structures*. RMS-8. Stanford, CA: Reliability of Marine Structures; 1990:70.
8. Cordova CACPP, Deierlein GG, Mehanny SSF. Development of a two-parameter seismic intensity measure and probabilistic design procedure. *J Eng Appl Sci*. 2001;51(2):233-252.
9. Baker JW, Jayaram N. Correlation of spectral acceleration values from NGA ground motion models. *Earthq Spectra*. 2008;24(1):299-317. <https://doi.org/10.1193/1.2857544>
10. Lin T, Haselton CB, Baker JW. Conditional spectrum-based ground motion selection. Part II: intensity-based assessments and evaluation of alternative target spectra. *Earthq. Eng. Struct. Dyn*. Oct. 2013;42(12):1867-1884. <https://doi.org/10.1002/eqe.2303>
11. Baker JW, Bradley BA. Intensity measure correlations observed in the NGA-West2 database, and dependence of correlations on rupture and site parameters. *Earthq Spectra*. 2017;33(1):145-156. <https://doi.org/10.1193/060716EQS095M>
12. Daneshvar P, Bouaanani N, Godia A. On computation of conditional mean spectrum in Eastern Canada. *J Seismol*. 2015;19(2):443-467. <https://doi.org/10.1007/s10950-014-9476-6>
13. Cimellaro GP. Correlation in spectral accelerations for earthquakes in Europe. *Earthq. Eng. Struct. Dyn*. Apr. 2013;42(4):623-633. <https://doi.org/10.1002/eqe.2248>
14. Chiou BJS, Youngs RR. An NGA model for the average horizontal component of peak ground motion and response spectra. *Earthq Spectra*. 2008;24(1):173-215. <https://doi.org/10.1193/1.2894832>
15. Ji K, Bouaanani N, Wen R, Ren Y. Correlation of spectral accelerations for earthquakes in China. *Bull Seismol Soc Am*. 2017;107(3):1213-1226. <https://doi.org/10.1785/0120160291>
16. Ji K, Bouaanani N, Wen R, Ren Y. Introduction of conditional mean spectrum and conditional spectrum in the practice of seismic safety evaluation in China. *J Seismol*. 2018;22(4):1005-1024. <https://doi.org/10.1007/s10950-018-9747-8>
17. Goda K, Hong HP. Spatial correlation of peak ground motions and response spectra. *Bull Seismol Soc Am*. 2008;98(1):354-365. <https://doi.org/10.1785/0120070078>

18. Hong HP, Goda K. Characteristics of horizontal ground motion measures along principal directions. *Earthq Eng Eng Vib*. 2010;9(1):9-22. <https://doi.org/10.1007/s11803-010-9048-x>
19. Jaimes MA, Candia G. Interperiod correlation model for Mexican interface earthquakes. *Earthq Spectra*. 2019;35(3):1351-1365. <https://doi.org/10.1193/080918EQS200M>
20. Singh SK, Mena E, Castro R. Some aspects of source characteristics of the 19 September 1985 Michoacán earthquake and ground motion amplification in and near Mexico City from strong motion data. *Bull Seismol Soc Am*. 1988;78(2):451-477. <https://doi.org/10.1017/CBO9781107415324.004>
21. Furumura T, Singh SK. Regional wave propagation from Mexican subduction zone earthquakes: the attenuation functions for interplate and inslab events. *Bull Seismol Soc Am*. 2002;92(6):2110-2125. <https://doi.org/10.1785/0120010278>
22. Singh SK, Reinoso E, Arroyo D, et al. Deadly intraslab Mexico earthquake of 19 September 2017 (Mw 7.1): ground motion and damage pattern in Mexico City. *Seismol Res Lett*. 2018;89(6):2193-2203. <https://doi.org/10.1785/0220180159>
23. Bojórquez E, Iervolino I, Manfredi G. Evaluating a new proxy for spectral shape to be used as an intensity measure. *AIP Conf. Proc*. 2008;1020(PART 1):1599-1606. <https://doi.org/10.1063/1.2963788>
24. Bojórquez E, Iervolino I. Spectral shape proxies and nonlinear structural response. *Soil Dyn Earthq Eng*. 2011;31(7):996-1008. <https://doi.org/10.1016/j.soildyn.2011.03.006>
25. Bojórquez E, Iervolino I, Reyes-Salazar A, Ruiz SE. Comparing vector-valued intensity measures for fragility analysis of steel frames in the case of narrow-band ground motions. *Eng Struct*. 2012;45:472-480. <https://doi.org/10.1016/j.engstruct.2012.07.002>
26. Buratti N. A comparison of the performances of various ground motion intensity measures. *15th World Conference on Earthquake Engineering*. Lisbon, Portugal; 2012.
27. Baker JW. Measuring bias in structural response caused by ground motion scaling. *Bull Seismol Soc Am*. 2006;19(1):1-6. <https://doi.org/10.1002/eqe>
28. Jamshidiha HR, Yakhchalian M, Mohebi B. Advanced scalar intensity measures for collapse capacity prediction of steel moment resisting frames with fluid viscous dampers. *Soil Dyn Earthq Eng*. 2018;109(March):102-118. <https://doi.org/10.1016/j.soildyn.2018.01.009>
29. Kazantzi AK, Vamvatsikos D. Intensity measure selection for vulnerability studies of building classes. *Earthq. Eng. Struct. Dyn*. Dec. 2015;44(15):2677-2694. <https://doi.org/10.1002/eqe.2603>
30. Kohrangi M, Bazzurro P, Vamvatsikos D, Spillatura A. Conditional spectrum-based ground motion record selection using average spectral acceleration. *Earthq. Eng. Struct. Dyn*. Aug. 2017;46(10):1667-1685. <https://doi.org/10.1002/eqe.2876>
31. Reyes C, Miranda E, Ordaz M, Meli R. Estimación de espectros de aceleraciones correspondientes a diferentes periodos de retorno para las distintas zonas sísmicas de la ciudad de México. *Rev. Ing. Sísmica*. 2002;121(66):95. <https://doi.org/10.18867/ris.66.198>
32. Jaimes MA, Reinoso E, Ordaz M. Comparison of methods to predict response spectra at instrumented sites given the magnitude and distance of an earthquake. *J. Earthq. Eng*. 2006;10(6):887-902. <https://doi.org/10.1080/13632460609350622>
33. Jaimes MA, Ramirez-Gaytan A, Reinoso E. Ground-motion prediction model from intermediate-depth intraslab earthquakes at the hill and lake-bed zones of Mexico City. *J Earthq Eng*. 2015;19(8):1260-1278. <https://doi.org/10.1080/13632469.2015.1025926>
34. García D, Singh SK, Herraiz M, Ordaz M, Pacheco JF. Inslab earthquakes of Central Mexico: peak ground-motion parameters and response spectra. *Bull Seismol Soc Am*. 2005;95(6):2272-2282. <https://doi.org/10.1785/0120050072>
35. Jayaram N, Baker JW. Statistical tests of the joint distribution of spectral acceleration values. *Bull Seismol Soc Am*. 2008;98(5):2231-2243. <https://doi.org/10.1785/0120070208>
36. Ordaz M, Singh SK, Arciniega A. Bayesian attenuation regressions: an application to Mexico City. *Geophys J Int*. 1994;117(2):335-344. <https://doi.org/10.1111/j.1365-246X.1994.tb03936.x>
37. Liu TJ, Pozos-Estrada A, Gomez R, Hong HP. Seismic hazard estimation: directly using observations versus applying seismic hazard model. *Nat Hazards*. 2016;80(1):639-655. <https://doi.org/10.1007/s11069-015-1988-z>
38. Hong HP, Pozos-Estrada A, Gomez R. Orientation effect on ground motion measurement for Mexican subduction earthquakes. *Earthq. Eng. Eng. Vib*. 2009;8(1):1-16. <https://doi.org/10.1007/s11803-009-8155-z>
39. CFE. *Manual de Diseño de Obras Civiles Diseño por Sismo*; 2015.
40. Carlton B, Abrahamson N. Issues and approaches for implementing conditional mean spectra in practice. *Bull Seismol Soc Am*. 2014;104(1):503-512. <https://doi.org/10.1785/0120130129>
41. García Jiménez D. Estimación de parámetros del movimiento fuerte del suelo para terremotos interplaca e intraslab en México Central. 159; 2006.
42. Kutner MH, Nachtsheim CJ, Neter J, Li W. *Applied linear statistical models*. New York: The McGraw-Hill Companies Inc.; 2005.
43. Lin T, Harmsen SC, Baker JW, Luco N. Conditional spectrum computation incorporating multiple causal earthquakes and ground-motion prediction models. *Bull. Seismol. Soc. Am*. 2013;103(2 A):1103-1116. <https://doi.org/10.1785/0120110293>
44. Bazzurro P, Cornell CA. Disaggregation of seismic hazard. *Bull Seismol Soc Am*. 1999;89(2):501-520.
45. Kramer SL. *Geotechnical Earthquake Engineering*. Prentice-Hall Civil Engineering and Engineering Mechanics Series. Upper Saddle River, NJ: Prentice Hall; 1996:653.
46. Esteva L. Regionalización sísmica de México para fines de ingeniería. Report 246, Universidad Nacional Autónoma de México, April 1970.

47. Ordaz M, Singh SK, Reinoso E, Lermo J, Espinosa JM, Dominguez T. Mexico earthquake of September 19, 1985—estimation of response spectra in the lake bed zone of the Valley of Mexico. *Earthq Spectra*. 1988;4(4):815-834. <https://doi.org/10.1193/1.1585504>
48. Singh SK, Lermo J, Domínguez T, et al. The Mexico earthquake of September 19, 1985—a study of amplification of seismic waves in the valley of Mexico with respect to a hill zone site. *Earthq Spectra*. 1988;4(4):653-673. <https://doi.org/10.1193/1.1585496>
49. Reinoso E, Ordaz M. Spectral ratios for Mexico City from free-field recordings. *Earthq Spectra*. 1999;15(2):273-295. <https://doi.org/10.1193/1.1586041>

How to cite this article: Rodríguez-Castellanos A, Ruiz SE, Bojórquez E, Reyes-Salazar A. Influence of spectral acceleration correlation models on conditional mean spectra and probabilistic seismic hazard analysis. *Earthquake Engng Struct Dyn*. 2021;50:309–328. <https://doi.org/10.1002/eqe.3331>